Proceedings of the 2010 3rd IEEE RAS & EMBS
International Conference on Biomedical Robotics and Biomechatronics,
The University of Tokyo, Tokyo, Japan, September 26-29, 2010

Active heart stabilization using adaptive noise cancelling techniques with gyroscopic actuation

Julien Gagne*†, Édouard Laroche*, Olivier Piccin*† and Jacques Gangloff*

***Abstract*— Active cardiac stabilization contributes to the development of less invasive surgical techniques in the cardiac field. We propose a device insuring this function by using the gyroscopic effect to generate the compensation torque. This solution avoids any linkage to the environment and allows to design a completely independant system, pluggable on commercial instruments. After presenting the principle and the design aspects, we focus on an adaptive approach for the control and how it can be combined with frequency estimation in order to cope with variable heart frequency. Finally we present experimental results highlighting the efficiency of the method with a 70% reduction of the displacements and a highly accurate cardiac frequency tracking.**

I. Introduction

A. Medical issues

The benefits introduced by recent less invasive surgical techniques like laparoscopic surgery are numerous: e.g. it reduces infectious hazard, scars size, hospital stay and patient recovery time. They are now widely used in particular for gastrointestinal, gynecological and urological surgery but their extension to other fields remains a great challenge. For instance in cardiac surgery the use of minimally invasive techniques is not applicable easily as pointed out in [1], even though it could heavily improve surgery quality. Indeed a common operation like coronary artery bypass implies heavy invasive steps such as sternum dissection, rib cage opening and extra corporeal circulation which are main complication sources and could be avoided using minimally invasive beating heart surgery. Nevertheless dealing with the heart motion is the main hindrance to the use of such techniques.

B. Previous solutions

However, some beating heart coronary bypasses have been performed by open and laparoscopic ways as in [2]. In these cases, the cardiac motion has been compensated using passive stabilizers which are constituted by a stiff rod maintaining the area of interest on the myocardium thanks to two pressure or suction fingers. But with these stabilizers the residual motion due to the device attachment flexibility is not negligible as highlighted in [3].

An alternative is to make the stabilization active and compensate for the heart action in real time thanks to the application of a force or torque on the stabilizer structure. A first device based on active compensation was developed by Bachta *et al.* [4], demonstrating the efficiency of active stabilization approach. This solution is particularly efficient for low frequencies but suffers from a limited bandwidth because of proximal actuation. In addition it requires the use of specific instruments. The solution presented herein is based on an alternative actuation method that focuses on higher frequencies which are the most problematic for surgeons. Moreover it is fully autonomous and is designed to be pluggable to existing commercial instruments while satisfying the sterilizabitity constraints.

For this purpose, we chose to take advantage of the gyroscopic effect. This mechanical property is known to allow the generation of torques without the need to be linked to the ground since it is based on inertial effects. Various applications using this concept can be found in the literature: stabilization systems for ships [5], attitude control in zero gravity environments for satellites [6] and submarine robots [7], antisismic building stabilization [8] and non-grounded haptic interface [9] for instance. This principle is usually used for rather large and heavy structures, however we propose to use it at a smaller scale, within the framework of cardiac stabilization for beating heart surgery. Moreover, since the system presented here is independent from the surgical instrument, the concept can be extended to other applications needing structure stabilization in similar frequency domain.

C. Problem technical specification

Since the system should compensate for heart actions, the corresponding forces have to be identified. For this purpose, assessment of forces applied on a passive stabilizer distal end were performed *in vivo* in real operation conditions on an anesthezied swine [4]. Force recording is presented in Fig. 1. The data revealed that force and displacements are prominent along the vertical direction confirming the results from [10]. Hence we chose to apply active compensation to the vertical axis. The measured forces vary in the range $0 - 3.5$ N so the gyroscopic system should be able to generate equivalent torque which is an entry point for the design. Frequency-domain data analysis highlighted several distinct actions: a constant value due to initial constraint needed to maintain the heart that prevents stabilizer unsticking, breathing components with a fundamental frequency of 0.25 Hz, and heart beating components starting at 1.5 Hz. In the sequel we will focus on the compensation of cardiac component only, which is the core of the problem. Indeed the breathing motion is not specific to cardiac surgery and surgeons are able to cope

*The authors are with the LSIIT Laboratory (UMR CNRS–UdS 7005), Pôle API, bd. Sébastien Brant, BP 10413, 67412 Illkirch CEDEX, FRANCE
†J. Gagne and O. Piccin are also with INSA of Strasbourg, 24 bd. de la Victoire, 67084 Strasbourg CEDEX, FRANCE
e-mails: gagne.julien@unistra.fr, laroche@unistra.fr, olivier.piccin@insa-strasbourg.fr, jacques.gangloff@unistra.fr

978-1-4244-7709-8/10/$26.00 ©2010 IEEE

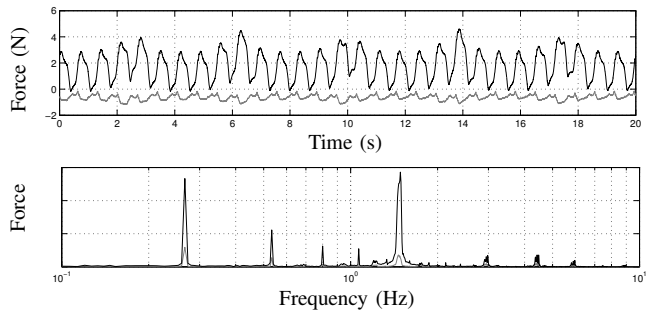

Fig. 1. Heart action recording in time (on top) and frequency (on bottom) domains. In black the vertical force component and in gray the horizontal one.

with it in most cases.

II. Device overview

A. Modeling

The designed gyroscopic compensation device and the passive stabilizer can be modeled using the rigid-body model which is depicted in Fig. 2. The compensation device is

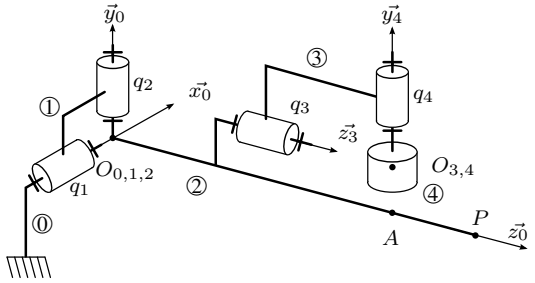

Fig. 2. Mechanical model in its reference configuration.

composed of an inertia wheel ④ rotating at a constant high speed Ω with respect to the joint q_4 thanks to a first actuator. This constitutes the gyroscope. This wheel is attached to a gimbal ③ which rotation with respect to the joint q_3 can be controlled with a second actuator. The whole system is attached to the passive stabilizer so that the gyroscope axis is aligned with A at its nominal position. The passive stabilizer is modeled by the part ② and its flexibilities are taken into account with the introduction of the massless part ① and the two revolute joints q_1 and q_2. Springs and dampers of coefficient k and f respectively are mounted on those two latter joints in order to model the properties of the flexibilities. Modeling flexibilities in this way is particularly relevant for our application since most deformations are concentrated in the stabilizer attachment and not distributed along the whole structure.

This architecture allows to compensate for displacements along the vertical axis $\vec{y_0}$ thanks to the gyroscopic torque generated along a direction parallel to $\vec{x_0}$. Let consider the gyroscopic torque expression:

$$\vec{T_G} = J_4 \vec{\Omega} \times \vec{R} \tag{1}$$

where $\vec{T_G}$ is the gyroscopic torque, $\vec{\Omega}$ the gyroscope angular velocity along its revolution axis, J_4 its moment of inertia and $\vec{R}$ the precession speed i.e. the gyroscope angular velocity normal to $\vec{\Omega}$. In order to obtain gyroscopic torque along $\vec{x_0}$ direction the vectors $\vec{\Omega}$ and $\vec{R}$ should be in the $(\vec{y_0}, \vec{z_0})$ plane. The configuration we chose fulfills this condition with $\vec{\Omega} = \Omega \vec{y_4}$ and $\vec{R} = \dot{q_3}\vec{z_3}$. It also avoids reverse undesired gyroscopic effects: displacements of the rod tip along $\vec{x_0}$ add a negligible variation to the gyroscope spinning rate and vertical displacements along $\vec{y_0}$ induce a torque along q_3 which can be handled by the actuator.

Considering that the displacements are small, neglecting gravity and minor gyroscopic effects, and considering only the vertical displacements, we demonstrated in previous work [11] that the system can be described by the following differential equation:

$$J\ddot{y} + f\dot{y} + ky = L\cos(q_3)T_G - L^2 F_y \tag{2}$$

$$T_G = J_4 \dot{q_3} \Omega \tag{3}$$

where y is the vertical displacement of the tip of the stabilizer, J the moment of inertia of the whole system, i.e. the stabilizer and the gyroscopic device, with respect to $\vec{x_0}$ axis, L the stabilizer length, and F_y the force exerted by the heart along the vertical direction.

According to equation (3) the gyroscopic torque T_G is proportional to the gimbal speed, the gyroscope speed and its moment of inertia. So it is possible to control the gimbal speed $\dot{q_3}$ so that it induces the appropriate torque required to compensate for heart motion in real time. Note that the gyroscope torque direction depends on the gimbal angle q_3 so the gimbal has to be kept close to its reference configuration in order to avoid gyroscopic torque along undesired direction.

B. Design issues

The compensator should be as compact and light as possible and able to produce a high gyroscopic effect. For this purpose we refer to equation (2) in which the gyroscopic torque is projected along $\vec{x_0}$. If we want to compensate for a cardiac action $F_y(t) = \frac{A_c}{2}\cos(2\pi f_c t)$ the gimbal angle expression will be the following:

$$q_3(t) = \arcsin\left(\frac{LA_c \sin(2\pi f_c t)}{4\pi J_4 \Omega f_c}\right) \tag{4}$$

The design choices are limited to the parameters J_4 and Ω which can be determinated based on the signal we want to compensate for and the boundaries constraints we impose on the gimbal angle. Finally we chose to maximize the gyroscope spin rate rather than its inertia which would induce higher weight.

Another important constraint on the design is to provide a device compatible with existing passive stabilizers and independant to allow separate sterilization. Most parts of the system are made of aluminum to improve lightness except the gyroscope which is made of steel to increase its inertia. The gyroscope and gimbal axis are both guided thanks to stainless steel bearings. Mechanical design was validated

after successful static and modal finite element analysis using a worst case scenario. A picture of the system designed to comply with the specifications is presented in Fig. 3.

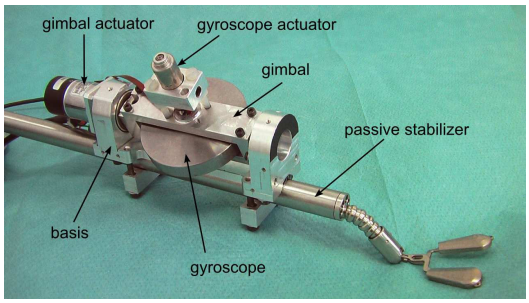

Fig. 3. System overview, here mounted on a passive stabilizer from Medtronic designed for minimally invasive beating heart surgery. The tip with the two fingers is inserted into the body while the gyroscopic system remains outside.

Finally the whole designed system is 130 mm long and weights 390 g. Thus, compactness is clearly improved compared to previous solutions, which makes the device easy to integrate in surgical environment. Concerning the performances, with a 30,000 rpm gyroscope spinning rate and $\pm 40°$ gimbal angle amplitude, the designed system is able to compensate for 1.5 Hz action with 5 N peak-to-peak amplitude, according to equation (4), which is sufficient considering cardiac force data.

C. Experimental setup

In order to evaluate the active stabilizer, we use the experimental setup depicted in Fig. 4. It is composed of the gyroscopic system attached to a stainless steel tube, which dimensions are similar to those of surgical stabilizers, and a heart simulator.

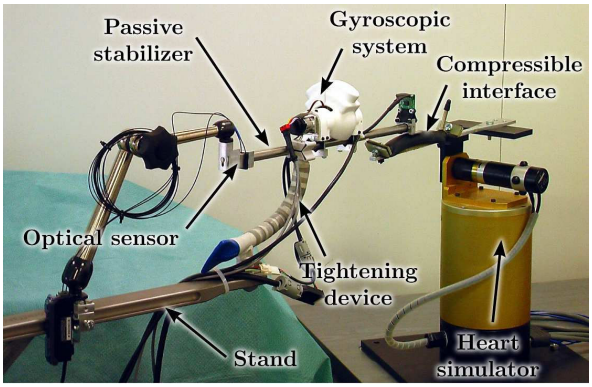

Fig. 4. Experimental setup overview.

The rod is attached thanks to a commercial system from Medtronic including a stand rigidly attached to the table and a cardiac stabilizer tightening device which presents some compliance. The heart simulator is composed of a pan-tilt robot which trajectory is controlled by a sequence reproducing the movements of a heart that were acquired experimentally on an anesthesized swine [12]. The contact between the heart simulator and the passive stabilizer is insured by a compressible interface which converts the imposed motion into force. The gyroscopic system actuators are controlled thanks to a real-time controller (Adept sMI6) which receives measurements from sensors and computes the control law with a sampling rate of 1 kHz. System monitoring is done from a laptop communicating with the controller trough firewire. It allows to set parameters, launch program sequences and make data acquisition.

Concerning the control of the gyroscopic device, various sensing solutions are possible: force, position, speed or acceleration sensors, camera. The accelerometer has many advantages: it can be easily embedded on the system, moreover, since its reference is inertial, it does not need any external component linked to the ground unlike a camera or position and speed sensors. Furthermore it does not require stabilizer modifications as for force sensing.

However, the presence of inaccuracies in the gyroscope manufacturing induces vibrations in the structure and high noise level on the acceleration measurement with amplitudes up to 15 times greater than the usefull signal [13], making the signal processing and the control difficult to implement experimentally. We are currently manufacturing a second version of the system with a special attention paid to the balance of the gyroscope in order to avoid any vibration. Nevertheless, in this paper, we want to validate a new adaptive control scheme which is independant from the type of measurement. Hence we chose to use for experiments a position sensor based on optical measurement. However this solution is not as ideal as acceleration sensing it is still pertinent within the application framework. The sensor is compact ($4 \times 11 \times 19$ mm) and is directly linked to the stand of the stabilizer with an articulated arm which allows an easy reconfiguration. The sensor is positionned on the proximal side of the stabilizer where it measures the displacements. Then, knowing the relationship between distal and proximal displacements, we deduct the stabilizer tip displacement. In addition, proximal measurement associated with no-contact optical sensing allows to respect the asepsis constraints.

In order to test and tune compensation control law in simulation, we need to identify the model parameters. For this, identification has been performed experimentally, based on mean square error minimization. Hence we were able to determine the values of the parameters of the gimbal local control loop and the passive stabilizer model [13].

III. Control strategies

A. Preliminaries

Using gyroscopic actuation to compensate for a disturbance requires the control law to fulfill a double objective:

1) reject the cardiac disturbance in order to stabilize the position y;
2) keep the gimbal close to its reference position to avoid a drift in torque direction.

One can note that these objectives are conflicting since gimbal angular displacement is necessary to generate torques. In

addition, the second constraint prevents to compensate for low frequency disturbance which would imply large gimbal angular displacements. So, according to the choice we made, i.e. to compensate for the cardiac frequencies but not for the breathing ones, the control law should allow compensation of frequencies higher than 1 Hz without compensating for lower frequencies.

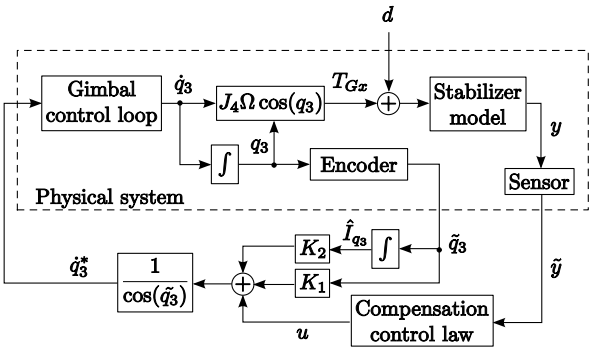

Fig. 5. Overall control scheme.

The overall control scheme is depicted in Fig. 5. In the sequel, we use the following notations: considering a signal x, $\hat{x}$ is an estimate, $\tilde{x}$ a measurement and x^* a reference value.

In order to satisfy the second objective, we chose to impose feedbacks on the gimbal angle measurement $\tilde{q}_3$ and its integral $\hat{I}_{q_3}$. The feedback on q_3 avoids gimbal drift while the one on I_{q_3} imposes an equilibrium position corresponding to the gimbal reference configuration [11]. Concerning the first objective, it is fulfilled thanks to a dedicated control law using a measurement $\tilde{y}$ and providing a control output u. This latter control law will be detailed in the sequel.

The system equation (2) includes the nonlinear term $\cos(q_3)$ in the gyroscopic torque expression. In order to compensate for this non linearity, we divide the control signal by $\cos(\tilde{q}_3)$ before sending it to the system input.

Finally the control input is defined in the following way:

$$\dot{q}_3^* = \frac{u + K_1\tilde{q}_3 + K_2\hat{I}_{q_3}}{\cos(\tilde{q}_3)} \tag{5}$$

where K_1 and K_2 are the feedback gains on $\tilde{q}_3$ and $\hat{I}_{q_3}$ respectively.

In a previous work [13], we studied compensation control laws using a Kalman observer for static state feedback and feedforward control. One limitation of those techniques in the need of an accurately identified model for the Kalman filter. In this paper we will focus on another approach based on adaptive control which is more tolerant to modeling uncertainties.

B. Adaptive control

In the case of cardiac motion compensation we know the frequencial content of the disturbance (cf. §I-C) which is constituted of the cardiac frequency and its harmonics. Since the cardiac frequency can slightly vary over time, we consider it as a time dependant signal ω remaining in the vicinity of a reference value ω^*. Finally the disturbance d can be considered as a sum of frequency varying sinusoidal disturbances of the form

$$d_i = A_i\cos(\varphi_i) \tag{6}$$

where $\varphi_i = \varphi_{i_0} + \int \omega_i \cdot dt$ with φ_{i_0} the initial value of φ_i and $\omega_i = i\omega$ the frequency of the i^{th} cardiac harmonic.

For input harmonic disturbance rejection Bodson and Douglas [14] proposed the adaptive control depicted in Fig. 6 which is based on the estimation of the amplitude of two components of the disturbance that are in phase quadrature to each other.

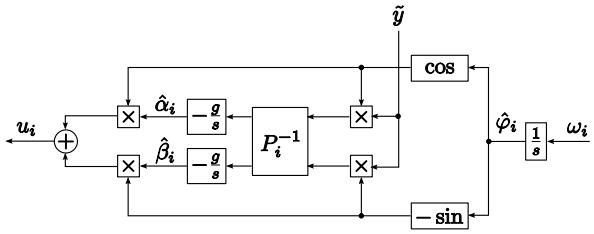

Fig. 6. Adaptive compensation control scheme for one harmonic.

Knowing the disturbance frequency ω the equation (6) can be writen in the following way:

$$d_i = \alpha_i\cos(\hat{\varphi}_i) - \beta_i\sin(\hat{\varphi}_i) \tag{7}$$

where $\hat{\varphi}_i = \int \omega_i \cdot dt$ is an estimate of φ_i. The gain g allows to tune the convergence speed of the algorithm and the gain matrix P_i^{-1} allows to compensate for the system gain and phase at the frequency ω_i^*. It is defined as:

$$P = \frac{1}{2}\begin{bmatrix} \mathrm{Re}[H(j\omega_i^*)] & -\mathrm{Im}[H(j\omega_i^*)] \\ \mathrm{Im}[H(j\omega_i^*)] & \mathrm{Re}[H(j\omega_i^*)] \end{bmatrix} \tag{8}$$

where $H(j\omega_i^*)$ is the transfer of the system from control input u to measurement $\tilde{y}$ at the working frequency ω_i^*. It corresponds to the system dynamic equation 2 with identified parameters. Then, the adaptive feedforward cancellation scheme leads to the control:

$$u_i = \hat{\alpha}_i\cos(\hat{\varphi}_i) - \hat{\beta}_i\sin(\hat{\varphi}_i) \tag{9}$$

For small values of g, the stability is guaranteed as long as the phase of $H(j\omega_i^*)$ is correctly estimated within a $\pm 90°$ tolerance. Hence this method is robust to model uncertainties. This robustness is an important advantage for our application since the properties of the system can be modified by the interaction with the heart or by a reconfiguration of the thightening device, to stabilize another part of the heart during an operation for instance. This method is also tolerant to gain errors since they would only have an influence on the convergence speed. Hence, complicated sensor calibration procedures can be avoided, leading to an simple use in operation conditions.

The scheme presented in Fig. 6 allows to compensate for only one harmonic disturbance. However it is possible to use

several samples of this scheme in parallel in order to compensate for more harmonics, using multiples of the cardiac frequency ω_i as inputs and defining the corresponding gain matrices P_i^{-1}.

C. Disturbance frequency estimation

Since the cardiac frequency ω is necessary for the adaptive control we need to measure or estimate it. This frequency information is generally not delivered directly by the commercial ECG devices. Even if the frequency can be obtained from cardiac electrical signals or ECG audible beeps, it is preferable to use the signals already available on the system so that it is completely independant from any other device.

For disturbance frequency estimation, Bodson and Douglas [14] recommand an adaptive notch filter derived from the one developed by Regalia [15]. It is compatible with the adaptive algorithm described in the previous subsection and uses as an input the same measurement as the adaptive algorithm. It has three states, x_1, x_2, and $\hat{\omega}$, that satisfy the following differential equations:

$$\dot{x_1} = x_2 \tag{10}$$

$$\dot{x_2} = -2\xi_e\hat{\omega}x_2 - \hat{\omega}^2 x_1 + k_e\tilde{y} \tag{11}$$

$$\dot{\hat{\omega}} = -g_e\left(k_e\tilde{y} - 2\xi_e\hat{\omega}x_2\right)x_1 \tag{12}$$

where the estimation gain g_e, the damping factor ξ_e and the filter gain k_e are positive constants to be tuned.

IV. Experimental results

A. Compensation with known frequency

We implemented on the experimental setup the adaptive algorithm and the frequency estimator described in the previous section. They were both tested first separately then together, imposing a cardiac-like action on the system thanks to the heart simulator.

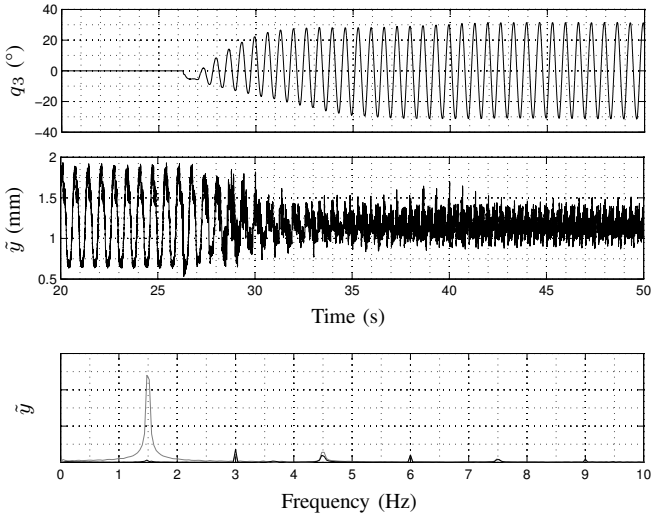

Fig. 7. Adaptive algorithm results with known cardiac frequency $\omega = 1.5$ Hz and $g = 0.5$. On top the gimbal angular displacement q_3 and in the middle the stabilizer measured displacement $\tilde{y}$. On bottom the comparison of the frequencial decomposition of the measured displacement $\tilde{y}$, with compensation ($t > 35$ s) in black and without ($t < 25$ s) in gray.

The results of the adaptive control with known disturbance frequency are shown in Fig. 7. Here only the compensation of fundamental at 1.5 Hz was implemented. The gain matrix P^{-1} was defined for this frequency, based on the identified model and we chose $g = 0.5$ which was the tuning presenting best performances in simulations.

The compensation was activated at $t = 26$ s. From there the control input, i.e. the gimbal speed $\dot{q_3}$, increases until the 1.5 Hz component is removed from the measurement signal $\tilde{y}$. One can see the compensation is effective within less than ten seconds. We can also observe at the very beginning of the compensation a lower frequency in the control input which corresponds to the phase matching. The gimbal centering is also effective, thanks to the feedback on q_3 and I_{q_3}, q_3 remaining centered around 0°, in a range of $\pm 30°$.

In terms of performances, the results show clearly the fundamental frequency attenuation. Compared to the free motion, we calculated a 70% reduction of the RMS amplitude of the displacement when compensation is active with 0.13 mm vs. 0.42 mm. However, the remaining displacements are mainly due to frequencies higher than the one we compensate for. This is confirmed by the frequencial decomposition of the displacement (lower plot) where we can see that the 1.5 Hz component is almost cancelled, higher frequencies being not affected.

So the proposed adaptive algorithm is able to efficiently reject an harmonic disturbance when its frequency is known. Let us now consider a variable frequency.

B. Including frequency estimation

We implemented the method presented in §III-C. The parameters were tuned in simulation in order to meet a good trade-off between convergence time and accuracy: $\xi_e = 0.1$, $k_e = 1000$ and $g_e = 1000$. In the experiment, the disturbance was activated suddenly at $t = 6$ s with a frequency varying between 1.4 and 1.6 Hz, while the frequency estimation was running from the beginning. The results are depicted in Fig. 8.

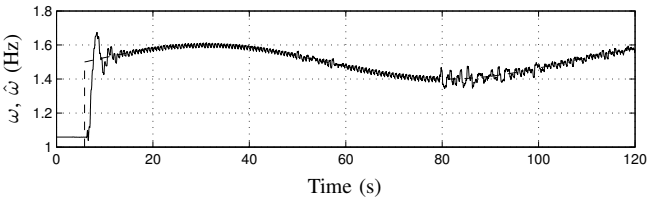

Fig. 8. Frequency estimation results. In dashed line the real pertubation frequency ω and in plain line its estimate $\hat{\omega}$. The frequency estimation parameters are the following: $\xi_e = 0.1$, $k_e = 1000$ and $g_e = 1000$.

We can observe the estimator converging to the real frequency within less than 10 s after the disturbance activation. Then, we can see the estimation remaining accurate and tracking the real frequency: we calculated a mean estimation error of 0.011 Hz which is less than 1% of the estimated frequency.

The results of the adaptive algorithm coupled with the frequency estimator are presented in Fig. 9. Here we impose a step on the disturbance frequency, switching from 1.5 to 1.6 Hz while compensation is active, the gain matrix P^{-1} being still defined for $\omega^* = 1.5$ Hz. This is a worst case scenario since in real conditions the heart frequency does not vary suddenly but progressively.

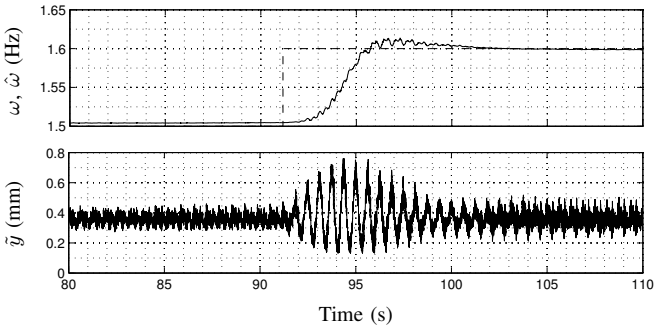

Fig. 9. Adaptive algorithm with frequency estimation results. On top the real perturbation frequency ω is in dashed line and the estimate $\hat{\omega}$ in plain line. On bottom the stabilizer displacement measurement $\tilde{y}$.

At the beginning the compensation is effective as in previous section since the frequency is well estimated. Then we observe a transition period of less than 10 s when both the frequency estimator and the adaptive algorithm have to fit the new conditions and during which the compensation is temporarily not effective. Afterwards the compensation settles again and the performances are recovered.

V. Conclusions and future work

The solution we propose to compensate actively for the heart displacement rely on the gyroscopic effect as an actuation mean. The principal advantage is the absence of linkage to the environment since it is based on an inertial effect. As a result, the designed device is entirely independant and pluggable on existing surgical heart stabilizers. Moreover, its design presents improvement concerning size, weight, surgical environment compatibility and ease of use while satisfying the constraints related to the surgical context.

The adaptive approach considered for the system control has several advantages. It is tolerant to uncertainties on the model and the measurement, well adapted to compensate for harmonic disturbances and can handle frequency variation when combined with cardiac frequency estimation.

The experimental results obtained prove the efficiency of the method for our application. The fundamental harmonic of the cardiac disturbance has been almost cancelled, resulting in a 70% reduction of the stabilizer displacement, the remaining motion being essentially due to non-compensated harmonics. The frequency estimator was able to track accurately the cardiac frequency allowing variable frequency compensation.

In future work, we plan to apply the adaptive algorithm to several harmonics in order to improve the performances. Then *in vivo* tests will be performed in order to validated the principle in real operation conditions. Another critical improvement would be the replacement of the position sensor by an accelerometer. This would allow to embed the whole compensation function and hence lead to a totally independant device. This requires to reduce the measurement noise, which could be done by minimizing the mechanical vibrations. For this purpose an improved prototype with high precision manufacturing for the gyroscope is being constructed.

VI. Acknowledgements

This work is supported by the Alsace Regional Council and the French National Center for Scientific Research (CNRS).

References

[1] M. J. Mack, "Minimally invasive cardiac surgery," *Surgical Endoscopy*, vol. 20, pp. 488–492, 2006.

[2] D. Y. Loisance, K. Nakashima, and M. Kirsch, "Computer-assisted coronary surgery: lessons from an initial experience," *Interact CardioVasc Thorac Surg*, vol. 4, no. 5, pp. 398–401, 2005.

[3] M. Lemma, A. Mangini, A. Redaelli, and F. Acocella, "Do cardiac stabilizers really stabilize? Experimental quantitative analysis of mechanical stabilization," *Interact CardioVasc Thorac Surg*, vol. 4, no. 3, pp. 222–226, 2005.

[4] W. Bachta, P. Renaud, E. Laroche, A. Forgione, and J. Gangloff, "Cardiolock: an active cardiac stabilizer, first in vivo experiments using a new robotized device," *Computer Aided Surgery*, vol. 13, no. 5, pp. 243–254, 2008.

[5] N. Townsend, A. Murphy, and R. Shenoi, "A new active gyrostabiliser system for ride control of marine vehicles," *Ocean Engineering*, vol. 34, no. 11-12, pp. 1607–1617, 2007.

[6] V. J. Lappas, W. H. Steyn, and C. I. Underwood, "Attitude control for small satellites using control moment gyros," *Acta Astronautica*, vol. 51, no. 1-9, pp. 101–111, 2002.

[7] B. Thornton, T. Ura, Y. Nose, and S. Turnock, "Zero-g class underwater robots: Unrestricted attitude control using control moment gyros," *Oceanic Engineering, IEEE Journal of*, vol. 32, no. 3, pp. 565–583, july 2007.

[8] H. Higashiyama, M. Yamada, Y. Kazao, and M. Namiki, "Characteristics of active vibration control system using gyro-stabilizer," *Engineering Structures*, vol. 20, no. 3, pp. 176–183, 1998, structural Control.

[9] H. Yano, M. Yoshie, and H. Iwata, "Development of a non-grounded haptic interface using the gyro effect," *11th Symposium on Haptic Interfaces for Virtual Environment and Teleoperator Systems, 2003. HAPTICS 2003. Proceedings.*, pp. 32 – 39, march 2003.

[10] P. Cattin, H. Dave, J. Grünenfelder, G. Szekely, M. Turina, and G. Zünd, "Trajectory of coronary motion and its significance in robotic motion cancellation," *Cardio-thoracic Surgery*, vol. 25, pp. 786–790, 2004.

[11] J. Gagne, O. Piccin, E. Laroche, and J. Gangloff, "A cardiac motion compensation device based on gyroscopic effect," *9th International Symposium on Robot Control (SYROCO'09)*, pp. 639–644, 2009.

[12] L. Cuvillon, J. Gangloff, M. de Mathelin, and A. Forgione, "Towards robotized beating heart tecabg : assessment of the heart dynamics using high-speed vision," *Computer Aided Surgery*, vol. 11, no. 5, pp. 267–277, September 2006.

[13] J. Gagne, O. Piccin, Édouard Laroche, and J. Gangloff, "A heart stabilization device exploiting gyroscopic actuation: design and control," *Proceedings of the ASME 2010 International Design Engineering Technical Conferences & Computer and Information in Engineering Conference IDETC/CIE 2010*, 2010.

[14] M. Bodson and S. C. Douglas, "Adaptive algorithms for the rejection of sinusoidal disturbances with unknown frequency," *Automatica*, vol. 33, no. 12, pp. 2213 – 2221, 1997.

[15] P. Regalia, "An improved lattice-based adaptive iir notch filter," *Signal Processing, IEEE Transactions on*, vol. 39, no. 9, pp. 2124 –2128, sep 1991.